land

MDPI

Article

Spatiotemporal Coupling of New-Type Urbanization and Ecosystem Services in the Huaihe River Basin, China: Heterogeneity and Regulatory Strategy

Muyi Huang [1,2,3,*], Qin Guo [4], Guozhao Zhang [1], Yuru Tang [4] and Xue Wu [1]

1. School of Environment and Energy Engineering, Anhui Jianzhu University, Hefei 230601, China; zhangguozhao@stu.ahjzu.edu.cn (G.Z.); w1317805274@stu.webvpn.ahjzu.edu.cn (X.W.)
2. Anhui Provincial Key Laboratory of Environmental Pollution Control and Resource Reuse, Hefei 230601, China
3. Anhui Institute of Ecological Civilization, Hefei 230601, China
4. School of Architecture and Urban Planning, Anhui Jianzhu University, Hefei 230601, China; guoqin@stu.ahjzu.edu.cn (Q.G.); tyr@stu.ahjzu.edu.cn (Y.T.)
* Correspondence: huangmuyi@ahjzu.edu.cn

Abstract: Strengthening the exploration of synergistic promotion mechanisms between ecosystem services (ESs) and new urbanization is of great significance for watershed development. In this work, we revealed the evolution mechanism of coupling coordination development degree (CCD) between ESs and new urbanization and its driving factors in the Huaihe River Basin (HRB) from 1980 to 2020 using a combination of the CCD model, Exploratory Spatial Data Analysis (ESDA) method, and GeoDetector model. Additionally, we employed the PLUS model to investigate multi-scenario simulations. The results demonstrate that ESs showed a decline initially, followed by an increase, while the urbanization index showed consistent annual growth over the four decades. Furthermore, the CCD between the ESs and urbanization showed a yearly optimization trend. The CCD demonstrated notable spatial clustering characteristics, with factors such as precipitation, distance from water body, elevation, and per area GDP emerged as the primary drivers. Under scenarios of ecological protection, comprehensive development, and natural protection, the value of ESs from 2020 to 2050 maintained an upward trend; however, it fell with the decrease under the scenario of cropland protection. These research findings offer valuable decision-making support for the differentiated regulation of ecosystem functions and promotion of high-quality urbanization development in the HRB.

Keywords: ecosystem services; urbanization; coupling coordination; scenario simulation; Huaihe River Basin

1. Introduction

The Huaihe River Basin (HRB) is a major base for food supply, energy, and manufacturing in China, and the main area for the implementation of the major strategy of the Rise of Central China. In 2018, the Development Plan of the HRB clearly positioned the region to create China's watershed ecological civilization construction demonstration belt, with the characteristics of industrial innovation and a development belt, a new urbanization demonstration belt, the central and eastern part of the cooperation, and development of the pioneering area [1]. At present, the HRB accounts for about one-sixth of the total national grain production and provides almost one-fourth of the state commodity grain. In the last 40 years, China's rapid urbanization has caused tremendous pressure and challenges to

the ecosystem [2–4]. Long-term agricultural production, industrial expansion, and swift urbanization have altered the landscape pattern of the watershed, impacting the ecosystem processes and functions therein. Consequently, the sustainable development of the HRB ecosystem has emerged as a prominent focus for both academics and policymakers [5]. Presently, the HRB is in a critical period of transition to high-quality development, while the health and stability of the ecosystem bear crucial implications for the basin's high-quality economic and social advancement [6]. Ecosystem services serve as a crucial link between natural ecosystems and socio-economic systems, encompassing these benefits, including water supply, air purification, soil conservation, food production, and cultural enrichment [7], ensuring human health and well-being [8–10]. Presently, the application of ecosystem services extends to various domains such as ecological health diagnosis, ecological product supply, ecological compensation [11], and ecological management [12]. However, these studies have predominantly explored ecological conservation issues from specific aspects or at specific socio-economic stages.

The scientific questions currently include how to establish a multidimensional evaluation framework to strengthen the integrated assessment of urbanization quality and ecosystem functions in the HRB. How can we effectively reveal the intrinsic coupling relationship between urbanization and ecosystem services and identify the dominant factors leading to spatial heterogeneity in the coupling results? Additionally, what regulatory strategies need to be designed to ensure the coordinated enhancement of ecological functions and urbanization quality in the HRB?

Currently, a significant number of studies on ecosystem services, based on models and methods such as the InVEST model, PLUS model, and Geodector model, have been conducted at various scales, including counties, cities, provinces, and river basins. These studies have become a focal point in the field. The analysis indicates that recent studies on the integration of ecosystem services and urbanization have primarily focused on counties, provinces, urban agglomerations, economic zones, and river basin units. Research hotspots include the Yangtze River Delta urban agglomeration [13], the Beijing–Tianjin–Hebei urban agglomeration [14], the Yangtze River Economic Belt [15], the Yellow River Basin [16], and the Yangtze River Basin [17]. Furthermore, relevant research has mainly focused on the following areas: (1) Based on the InVEST model and the coupled coordination degree model, exploring the coupling and coordination of urbanization and ecosystem services (single or multiple ecosystem services), with a view to realizing the sustainable development of the region [18,19]. (2) Adopting the coupled coordination degree model and geographically weighted regression (GWR) model to explore the relationship and influence mechanism of urbanization and socio-economic systems [20]. (3) Adopting the spatial autocorrelation model and the PVAR model to analyze the coupling relationship and dynamic influence mechanism of new urbanization and ecological resilience, so as to explore the coordinated development strategy of social-ecological systems [21]. (4) In the context of the reality of new urbanization, constructing a comprehensive evaluation model of new urbanization and ecological environment, and carrying out research on the interaction relationship and mechanism of action between the two [22]. (5) Based on panel data, the spatial correlation between the value of ecosystem services and urbanization has been revealed by constructing a comprehensive evaluation model of the two [23]. (6) The PLUS model has been used to explore the mechanisms of spatiotemporal changes in the interaction between ecosystem services and urbanization under different scenarios [17]. In general, existing studies have explored the relationship between ecosystem services and urbanization in depth. However, in the HRB, China, research based on a multidimensional framework for new urbanization and ecosystem services evaluation, focusing on the spatial heterogeneity of coupling coordination development degree (CCD) and employing multi-

scenario methods, with targeted strategic recommendations for basin development, remains relatively scarce.

Therefore, the aim of this study is to fill these gaps. The specific objectives include the following: (1) introducing a multidimensional new urbanization indicator system for the HRB; (2) identifying the dominant factors in the CCD through GeoDetector analysis and unveiling its driving mechanisms; and (3) proposing a differentiated regulatory approach and a strategic implications consisting of "one framework, two methods, and three pathways" based on multi-scenario simulation analysis.

2. Materials and Methods

2.1. Study Area

The HRB (30°31′ N–37°17′ N, 112°45′ E–120°88′ E) is situated in the eastern region of China. It extends from the Tongbai and Funiushan Mountains in the west and borders the Yellow Sea in the east. To the north, it shares boundaries with the Yellow River Basin. The study area encompasses 40 prefectural-level cities and 316 counties and district units across Anhui, Jiangsu, Henan, Shandong, and Hubei provinces (Figure 1). Covering an area of about 39.25×10^4 km^2, the HRB serves as a crucial hub for economic development and agricultural production in China. It boasts a diverse industrial structure, well-developed waterway transportation, and a rich historical and cultural heritage. Functioning as a distinctive north–south transition zone, the basin constitutes a unique ecological corridor in China. During the 1980s and 1990s, the Huai River suffered from severe pollution issues.
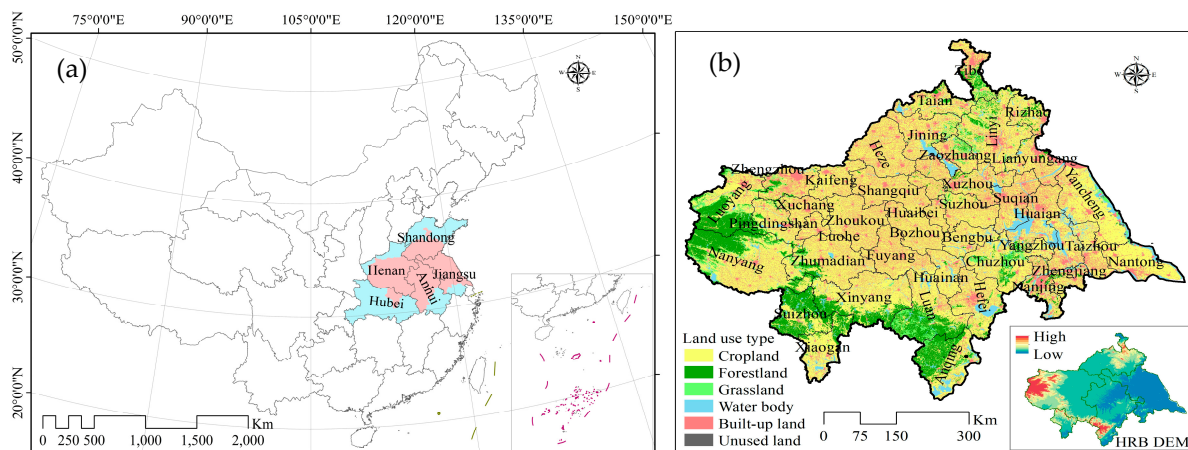

Figure 1. Scope of the study area (**a**) and information on its land use and DEM (**b**).

2.2. Data Sources and Processing

The data sources used in this work consisted of raster data, vector data, and statistical data in the HRB. Raster data mainly consisted of land use classification maps for the years 1980, 1990, 2000, 2010, and 2020. To align with the study's requirements, the land use types were reclassified into six categories: cropland, forestland, grassland, water body, built-up land, and unused land. Urbanization indicators (including urbanization rate (%), population density, number of registered urban unemployed individuals, economic growth rate, the proportion of secondary and tertiary industries in GDP, total retail sales of social consumer goods as a percentage of GDP (%), per capita GDP (CNY), built-up area, per capita park green area (m^2/person), urban built-up land area, the number of urban basic medical insurance participants, the number of urban workers participating in basic pension insurance, number of urban general institutions of higher learning) were obtained from various sources, including the China Urban Statistical Yearbook, Provincial

Statistical Yearbooks (Anhui, Jiangsu, Shandong, Henan, and Hubei), and relevant local and municipal Statistical Yearbooks and statistical bulletins spanning the years 1981–2021.

GeoDetector factor data and PLUS multi-scenario simulation indicators include DEM data (Geospatial Data Cloud with a 90 m resolution), meteorological data (rainfall, air temperature), population density, and per area GDP (raster data with a 1 km resolution). Distance to traffic and watershed data were acquired from OpenStreetMap and processed through Euclidean distance analysis in ArcGIS. Each factor generated a raster layer, subsequently discretized into the required data types for GeoDetectors. The information on the data is presented in Table 1.

Table 1. Information on the data.

Data Type	Variables	Year	Spatial Resolution	Unit	Data Sources
Land use data	land use classification maps	1980, 1990, 2000, 2010, and 2020	30 m	/	(https://www.resdc.cn/) (acessesd on 18 May 2024)
Natural factors	DEM	2000	90 m	m	(https://www.gscloud.cn/) (acessesd on 18 May 2024)
	slope	2000	90 m		DEM-based extraction
	aspect	2000	90 m		DEM-based extraction
	annual average temperature	2020	1000 m	0.1 °C	(https://www.resdc.cn/) (acessesd on 15 May 2024)
	annual average precipitation	2020	1000 m	0.1 mm	
	soil type	1995	1000 m	/	(https://www.resdc.cn/) (acessesd on 15 May 2024)
	distance from water body	2020	300 m	m	(https://www.openstreetmap.org/) (acessesd on 10 May 2024)
Socio-economic factors	population density	2019	1000 m	Persons/km^2	(https://www.resdc.cn/) (acessesd on 15 May 2024)
	GDP per area	2020	1000 m	10,000 CNY/km^2	
	distance from railroads	2020	/	/	(https://www.openstreetmap.org/) (acessesd on 10 May 2024)

2.3. ES Value

Land Use/Cover Changes (LUCCs) are a response to the complex coupling between human socio-economic activities and the land ecosystems. Globally, LUCCs are an important driver of ecosystem services and biodiversity change. In this study, the equivalence factor approach, proposed by a previous author [24,25], was used to assess the value of ecosystem services in the HRB. This method involves the classification of ESs into four primary and nine secondary categories. For the calculation of ESs for different years, the same equivalence factor coefficients were typically applied across all periods. The approach for determining the equivalence factor coefficients was as follows: the food supply value of cropland was first calculated using relevant statistical data, such as crop yields and grain prices, from the same period as the land use data (obtained from statistical yearbooks). Then, equivalence factor coefficients for other land use types were determined by comparing their relative importance. Finally, the ecosystem service value was calculated by multiplying the equivalence factor coefficients with the area of each land use type.

The evaluation of the ES value involves extracting the land use area in the unit across different years and scales. The ESs provided by each land ecosystem within the evaluation unit are then calculated individually, as outlined in Table 1. The total ES value for the evaluation unit is then determined, and is calculated as follows:

$$E_a = \sum_{i=1}^{n} \frac{m_i q_i p_i}{M} \tag{1}$$

where E_a represents the economic value of the unit area of cropland ecosystems providing the food production services function; n denotes the number of crop types, specifically selected as wheat, corn, soybeans, and rice; p_i signifies the average market price for the representative food crop of type i; q_i is the output per unit area of the i-th grain crop; m_i stands for the area of the i-th grain crop; M represents the total area of the n grain crops.

We derived the actual market prices of various grain crops from the Provincal Statistical Yearbooks and other sources. Specifically, the market prices for wheat, corn, soybeans, and paddy rice were 1.442 CNY/kg, 1.224 CNY/kg, 3.364 CNY/kg, and 1.373 CNY/kg, respectively. The average grain yield (3442.3029 kg/hm^2) and market price (1.855 CNY/kg) of arable land in the HRB from 1980 to 2020 were measured. For the calculation method, we refer to the relevant literature [26].

$$E_{ij} = A_{ij}/e_{ij} \tag{2}$$

where E_{ij} is the total unit value of the ES function i of the ecosystem category j; A_{ij} is the total area of the ecosystem category j; e_{ij} is the equivalence factor of the ES function i of the ecosystem category j.

Each service category was assigned an equivalence factor, where the ES value equivalent factor per unit area of cropland food production was assumed to be 1. The relevant equivalent factors of ESs in the HRB are provided in Table 2.

Table 2. Equivalent factor table of ES value per unit area in the HRB (CNY·hm^{-2}·a^{-1}).

Service Type		Land Type				
Level 1 Type	Level 2 Type	Cropland	Forestland	Grassland	Water Body	Unused Land
Supply services	food production	543.39	124.17	147.53	322.10	4.92
	raw material production	120.48	285.22	218.83	179.49	14.75
	water resources supply	−641.74	147.53	120.48	2675.16	9.84
	subtotal	22.13	556.92	486.84	3176.75	29.51
Regulation services	gas regulation	437.66	938.03	764.68	656.50	54.09
	climate adjustment	228.67	2806.71	2023.58	1448.23	49.18
	purification	66.39	822.46	668.79	2249.79	152.44
	environmental hydrology	735.18	1836.71	1482.65	31,096.29	103.27
	subtotal	1467.9	6403.91	4939.70	35,450.81	358.98
Support services	soil conservation	255.71	1142.11	931.88	796.65	63.93
	nutrient cycling	76.22	87.29	71.30	61.47	4.92
	biodiversity	83.60	1040.07	848.28	2562.06	59.01
	subtotal	415.53	2269.47	1851.46	3420.18	127.86
Cultural services	esthetic landscape	36.88	456.11	373.74	1627.72	24.59
	subtotal	36.88	456.11	373.74	1627.72	24.59
	total	1942.44	9686.41	7651.74	43,675.46	540.94

Note: Due to water consumption from planting and irrigation, the coefficient of water resources supply in cropland is negative.

2.4. Comprehensive Index Method and Coupling Coordination Degree

Precisely delineating and understanding the connotation and mechanism of coupling coordination between ESs and new urbanization is fundamental for advancing research on the synergistic advancement of high-quality development in the HRB (Figure 2). Through the lens of the mutual coupling mechanism between the two, urbanization exerts spatial influence on ecosystem dynamics, while the efficacy of ecosystem functioning reciprocally impacts the quality of urbanization. Improvements in urbanization quality provide financial support, cutting-edge technical assurance, and various control methods for environmental governance. Meanwhile, a high-quality ecological environment offers favorable ecological conditions and spatial frameworks for urbanization. These two aspects are interconnected and mutually reinforcing (Figure 2). Consequently, strengthening the response mechanism of ecosystem function to urbanization and exploring countermeasures for regulating ecosystem functions are a pivotal focus in coupling research. Additionally, the careful selection of urbanization indicators is crucial for evaluation. Based on the work of esteemed scholars [27], this study follows the principles of data accessibility, operability, representativeness, and scientific rigor, aligning them with the current conditions of the study area. Indicators were carefully selected from the domains of demographic evolution, socioeconomics, and spatial expansion to establish an index system for new urbanization development in the HRB (Table 3). A comprehensive index method was employed to evaluate the comprehensive index of new urbanization in the HRB. To eliminate the impact of different data dimensions on the evaluation results, this paper normalized the data for each index and determined the weight of each evaluation index using the entropy method [28]. Finally, the weighted summation method was used to calculate the new urbanization index.

$$U_i = \sum_{j=1}^{m} (U_{ij} \cdot \omega_{ij}) \tag{3}$$

where U_i is the comprehensive index of new urbanization at unit i; U_{ij} is the j-th indicator's standardized value at unit i; ω_{ij} is the j-th indicator's weight at the i-th unit.
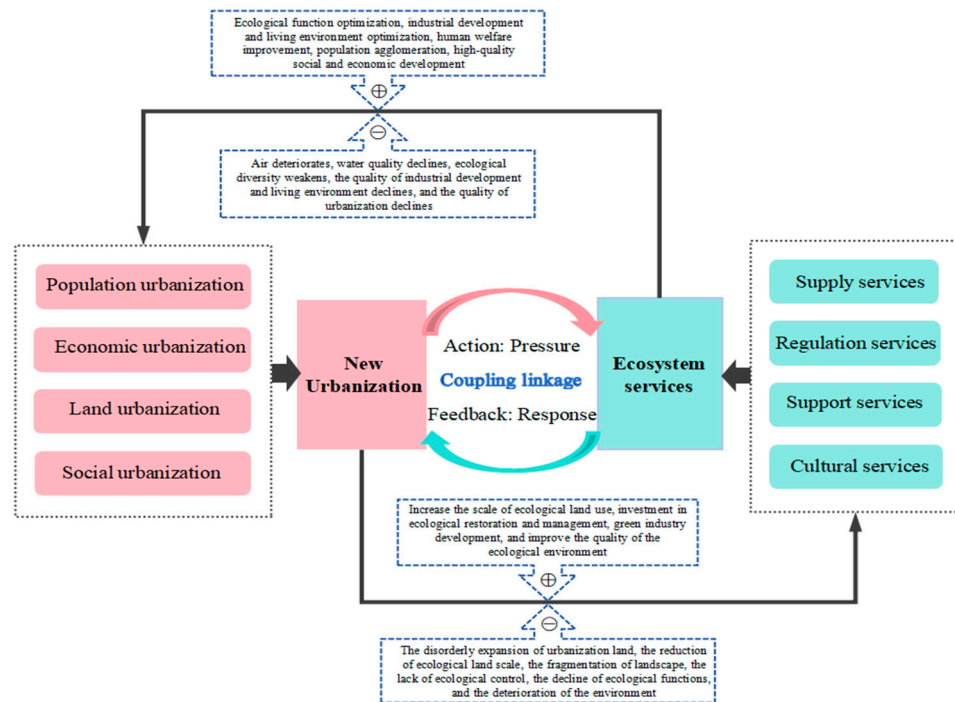

Figure 2. The connotation and path of the coupling effect between ESs and new urbanization.

Table 3. Index system of new urbanization in the HRB.

Target Layer	Classification Layer	Indicator Layer (Code and Name)	Indicator Attribute	Weight
U The urbanization index	U_p	U_{p1} Urbanization rate (%)	(+)	6.60%
		U_{p2} Population density	(−)	0.28%
		U_{p3} Number of registered urban unemployed individuals	(−)	0.35%
	U_e	U_{e1} Economic growth rate	(+)	0.41%
		U_{e2} The proportion of secondary and tertiary industries in GDP (%)	(+)	2.32%
		U_{e3} Total retail sales of social consumer goods as a percentage of GDP (%)	(+)	2.19%
		U_{e4} Per capita GDP (yuan)	(+)	17.70%
	U_l	U_{l1} Built-up area	(+)	11.98%
		U_{l2} Per capita park green area (m²/person)	(+)	11.92%
		U_{l3} Urban built-up land area	(+)	12.58%
	U_s	U_{s1} The number of urban basic medical insurance participants	(+)	8.77%
		U_{s2} The number of urban workers participating in basic pension insurance	(+)	10.28%
		U_{s3} Number of urban general institutions of higher learning	(+)	14.62%

The new urbanization index system was structured into three layers: the target layer, classification layer, and indicator layer. Each layer includes specific elements and indicators that contribute to the comprehensive assessment. The target layer, denoted as U for urbanization, consists of sub-indices related to population urbanization (Up), economic urbanization (Ue), land urbanization (U_l), and social urbanization (Us). Each sub-index was further broken down into specific indicators with associated weights.

After completing the assessment of the ecosystem service value and comprehensive urbanization, this study adopted the CCD model to calculate the level of interaction between the comprehensive index of ESs and the new urbanization index, in order to measure the CCD between the two. Given the limitations of the traditional coupling degree model [29], this study employed an improved coupling coordination model [30] to evaluate the coupling coordination status of ecosystem services and urbanization. The modified model ensures better coupling validity and credibility of the calculation results [31]. All formulas are as follows:

$$C = \sqrt{\left[1 - \frac{\sum_{i>j,j=1}^{n} \sqrt{(E_i - U_j)^2}}{\sum_{m=1}^{n-1} m}\right] \cdot \left(\prod_{i=1}^{n} \frac{EU_i}{\max EU_i}\right)^{\frac{1}{n-1}}} \tag{4}$$

$$T = \alpha \times E + \beta \times U \tag{5}$$

$$D = (C \times T)^{\frac{1}{2}} \tag{6}$$

where C is the coupling degree; n is the number of subsystem dimension; EU_i and EU_j are the subsystem dimension i and dimension j, respectively; $maxEU_i$ is the maximum value in the subsystem dimension.

To avoid a low-quality coupling situation with a high *C* value, the coupling degree model was utilized to calculate the CCD, expressing the quality of the coupling. *T* is the comprehensive coordination index between the two subsystems; α, β, respectively, are the ecosystem services and new urbanization comprehensive index of the weight value, where $\alpha + \beta = 1$. Referring to the relevant literature [32], the coupling quality was categorized into intervals such as (0.00, 0.10], (0.10, 0.19], (0.19, 0.29], (0.29,0.39], (0.39,0.49], (0.49,0.59], (0.59,0.69], (0.69,0.79], (0.79,0.89], and (0.89,1.00], representing high dysfunctionality, severe dysfunctionality, moderate dysfunctionality, mild dysfunctionality, verging on dysfunctionality, barely coordination, primary coordination, moderate coordination, good coordination, and high-quality coordination, respectively.

2.5. GeoDetector

The GeoDetector is mainly based on the spatial heterogeneity parameters of different layers (including layers of the independent variable and dependent variable) to detect the driving mechanism and measure the explanatory ability of the independent variable to the dependent variable through the *q*-value. When $q = 0$, it means that the independent variable has no influence on the dependent variable. When $q = 1$, it shows that the dependent variable is completely controlled by the change in the independent variable [33]. The q value is calculated as follows:

$$q = 1 - \frac{1}{N\sigma^2} \sum_{n=1}^{M} N_h \sigma_h^2 \tag{7}$$

where $h = 1, 2, ...$; *M* is the categorization of *Y* (dependent variable) or factor X (independent variable); N_h and N are the number of grid units in stratum *h* and the whole area, respectively; σ_h^2 and σ^2 are the variances in *Y* in layer *h* and the whole area, respectively.

The interaction detector compares a single factor with a two-factor interaction based on the *q*-value to characterize the interaction between two variables. This method is not confined to traditional statistical methods, offering advantages in identifying common interactions between drivers. The results can be used to identify whether co-interaction between independent variables enhances or weaken the ability to explain dependent variables [34].

2.6. Multi-Scenario Simulations

2.6.1. Principles of PLUS Simulation Model

The PLUS (Patch-generating Land Use Simulation, PLUS) model combines cellular automata with a patch-generation simulation strategy, significantly improving the model's ability to simulate real landscape patterns with high precision and enhancing the accuracy of simulation predictions. It also reveals the complex nonlinear interactions between land use changes and their influencing factors [35–37]. In this study, we aim to calculate the total ecosystem service (ES) value based on the simulated land use data. To achieve this, we first applied the PLUS model to simulate land use changes in the study area. First, the LEAS (land expansion analysis strategy, LEAS) module was used to extract the land expansion maps for various land types between 2010 and 2020. By inputting the extracted expansion maps and driving factor data into the LEAS module, development potential maps for each land type were generated. Simultaneously, the model parameter file automatically calculated the contribution of driving factors to the changes in each land type. Next, in the CARS (cellular automaton model based on multitype random patch seeds, CARS) module, the development potential maps and spatial policy constraint data were input. By considering land use type conversions across the study area, parameters such as the cost matrix and neighborhood weights were set. After iterative adjustments and debugging, the

final simulation results for future land use changes in the HRB under multiple scenarios were obtained.

2.6.2. Neighborhood Coefficient and Multi-Scenario Setup for PLUS Model

From the perspective of natural and socio-economic dimensions, GDP, population, temperature, precipitation, soil type, slope, aspect, distance from water body, distance from railroad, etc., were selected as the driving factors for the PLUS model. We compared the results of the PLUS simulation of land use data in 2020 with the actual data in 2020. If the simulation accuracy met the required standards, it could be used to simulate future land use changes under four scenarios in 2050. Neighborhood weight parameters represent the expansion intensity of different land use types (Table 4). The setting of weight parameters for land use in this paper was based on the relevant literature [38].

$$X_i = \frac{\Delta TA_i - \Delta TA_{\min}}{\Delta TA_{\max} - \Delta TA_{\min}} \tag{8}$$

where X_i is the neighborhood weight parameter of a land class i, ΔTA_i is the amount of change in *TA* of the land class, ΔTA_{min} is the minimum change, and ΔTA_{max} is the maximum change in *TA* over the past four decades.

Table 4. Neighborhood factor parameter settings for the PLUS model.

Land Use Type	Cropland	Forestland	Grassland	Water Body	Built-Up Land	Unused Land
Domain factor parameters	0.33	0.12	0.09	0.22	1	0

In this study, four distinct conversion matrices were developed to reflect the characteristics of land use type conversion under different scenarios.

(1) In the natural development (ND) scenario, the conversion cost matrix was set by allowing free conversions between cropland, forest, grassland, water bodies, and unused land. (2) In the cropland protection (CP) scenario, higher conversion costs (or lower conversion coefficients) were set for cropland in the conversion cost matrix to restrict its conversion to other land use types. (3) In the ecological protection (EP) scenario, a conversion cost matrix was constructed that tended to facilitate conversions between land use types with higher ecological value, such as forests, grasslands, and water bodies, while restricting their conversion to land use types with lower ecological value. (4) In the comprehensive development optimization (CD) scenario, the goal was to balance conversion costs while limiting the excessive expansion of grassland, forest, water bodies, and urban areas. Constraints were applied to urban expansion, promoting cropland development and ecological protection. The conversion cost matrix in this scenario was designed to reflect a more comprehensive and sustainable land planning and resource management strategy. The specific conversion matrix is shown in Table 5.

Finally, to evaluate the performance of land use change simulation results in the HRB, this study employed the Figure of Merit (FoM) evaluation method. FoM is defined as the ratio of the intersection of observed and simulated changes to the union of observed and simulated changes, serving as a metric for assessing the accuracy of the dynamic changes in the simulation outcomes [39]. Previous research has demonstrated that the FoM coefficient

is more suitable than the Kappa coefficient for evaluating the accuracy of land use and land cover (LULC) simulations [40]. The formula for calculating FoM is as follows:

$$FoM = B/(A + B + C + D) \tag{9}$$

where A represents the area where actual changes occurred but no changes were simulated; B denotes the area where both the actual and simulated results exhibited changes, with consistent directional shifts; C refers to the area where both the actual and simulated results showed changes, but with inconsistent directions of change; D represents the area where no actual change occurred, yet the simulation indicated change.

Table 5. Conversion cost matrix.

	ND						CP						EP						CD					
	A	B	C	D	E	F	A	B	C	D	E	F	A	B	C	D	E	F	A	B	C	D	E	F
A	1	1	1	1	1	1	1	0	0	0	0	0	1	1	1	1	1	1	1	0	0	1	1	1
B	1	1	1	1	1	1	1	1	1	0	0	1	0	1	0	0	0	0	1	1	1	0	0	0
C	1	1	1	1	1	1	1	1	1	1	1	1	1	0	1	1	1	0	0	1	1	1	1	1
D	1	1	1	1	1	1	1	0	1	1	0	0	0	0	1	0	0	0	0	1	1	0	0	0
E	0	0	0	0	1	0	0	0	0	0	1	0	0	0	0	0	1	0	0	0	0	0	1	0
F	1	1	1	1	1	1	1	1	1	1	1	1	1	1	1	1	1	1	1	1	1	1	1	1

Note: A, B, C, D, E, and F are cultivated land, forest land, grassland, water body, construction land, and unused land, respectively; 0 means that they cannot be converted, and 1 means that they can be converted.

2.7. Technology Roadmap
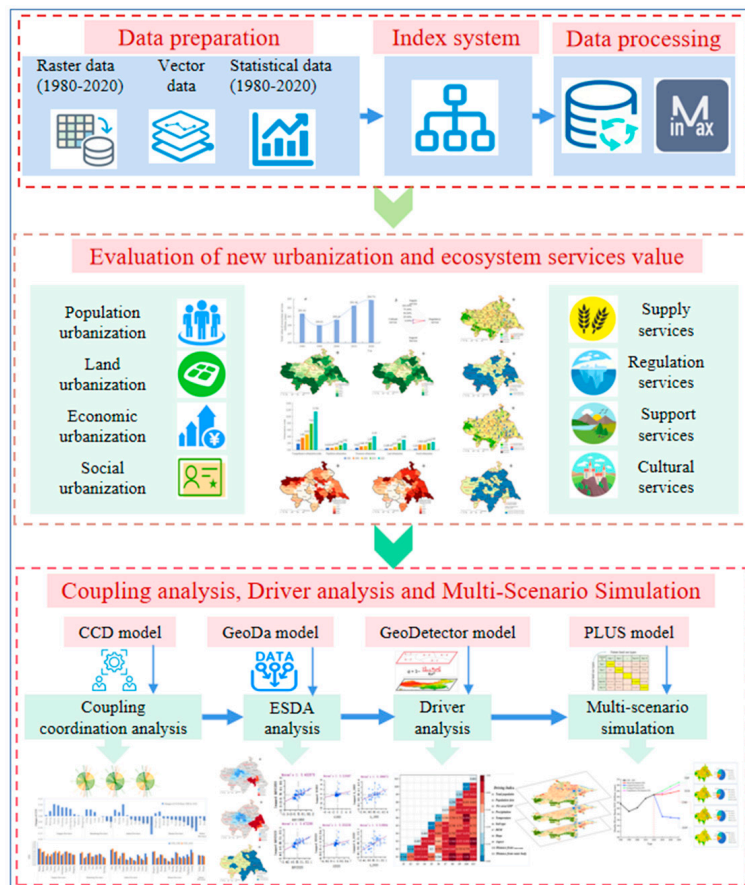
A technical roadmap of this research is shown in Figure 3.

Figure 3. Technical roadmap.

3. Results

3.1. Dynamic Analysis of the ES Value and New Urbanization

3.1.1. Spatial–Temporal Variation Characteristics of ES Value

The temporal analysis shows that from 1980 to 2020, the total ES value in the HRB presents a "V"-type variation characteristic of "first decreasing and then increasing", and the inflection point of change appears in 1990. Before this, the value of ESs decreased from CNY 201.63 billion in 1980 to CNY 199.01 billion in 1990. It rose to CNY 200.23 billion in 2000 and ultimately reached CNY 204.74 billion by 2020 (Figure 4a). Overall, from 1980 to 2020, the total ES value in the HRB increased by CNY 3.11 billion. When analyzed by stages, from 2000 to 2010, the total ES value increased by CNY 3.23 billion, while from 2010 to 2020, it only increased by CNY 1.27 billion, about 40% of the previous development stage, indicating a significant slowdown in the growth rate (Figure 4a). This dynamic trend exhibits clear temporal characteristics. Between 1980 and 2000, as urbanization and industrialization advanced in the HRB, large areas of cropland were converted into urban and industrial land, which significantly impacted ecosystem services such as water retention, soil conservation, and air purification, leading to a decline in ecosystem service value. Land use changes, policy measures, climate change, socio-economic development, and technological progress are interconnected and collectively influence the fluctuations in ecosystem service values in the HRB.
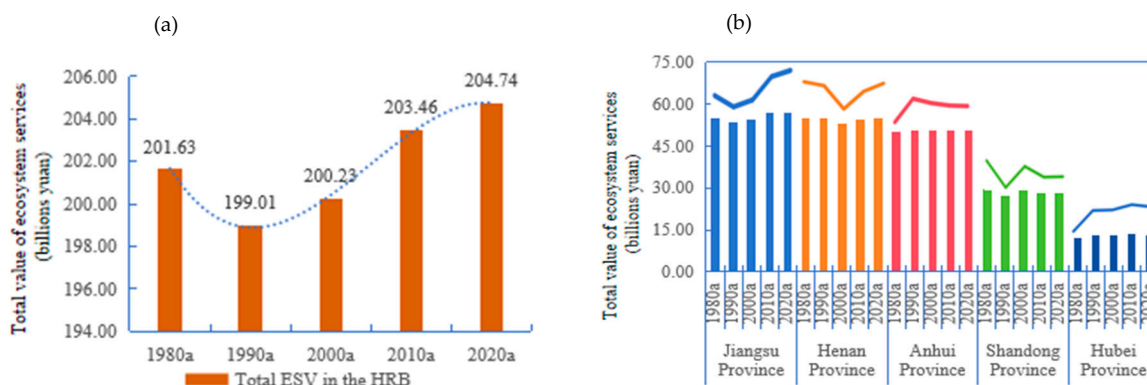
(a)   (b)

Figure 4. The temporal change in total ESV in the HRB from 1980 to 2020 (**a**), and the comparison of Provincial variation in total ESV (**b**).

At the provincial scale, it can be observed that the Jiangsu, Henan, and Anhui provinces are important contributors to ecosystem services in the HRB. The changes in the total ES value in these provinces show different development trends (Figure 4b).

There are distinct spatial characteristics in the ES values (ESVs) of 40 cities in the HRB (Figure 5). From 1980 to 2020, the spatial pattern of ESVs in the HRB remained relatively stable. The regions with a high ES value are located in the west and southeast of the HRB, while the regions with a low ES value are in the middle of the HRB (Figure 5a,b). The map of land use classification shows that the forest resources in the west HRB are abundant, and the water system in the southeast part of the HRB is well-developed (Figure 5c), so the ESV in the region is high. In contrast, the central region is primarily characterized by cropland, and the distribution of ESVs show a noticeable decline (Figure 5c). The analysis indicates significant spatial differences in the change in ESVs, in which the eastern and western parts of the basin were increasing areas of ecosystem service value, while the central part comprised the declining area (Figure 5d).
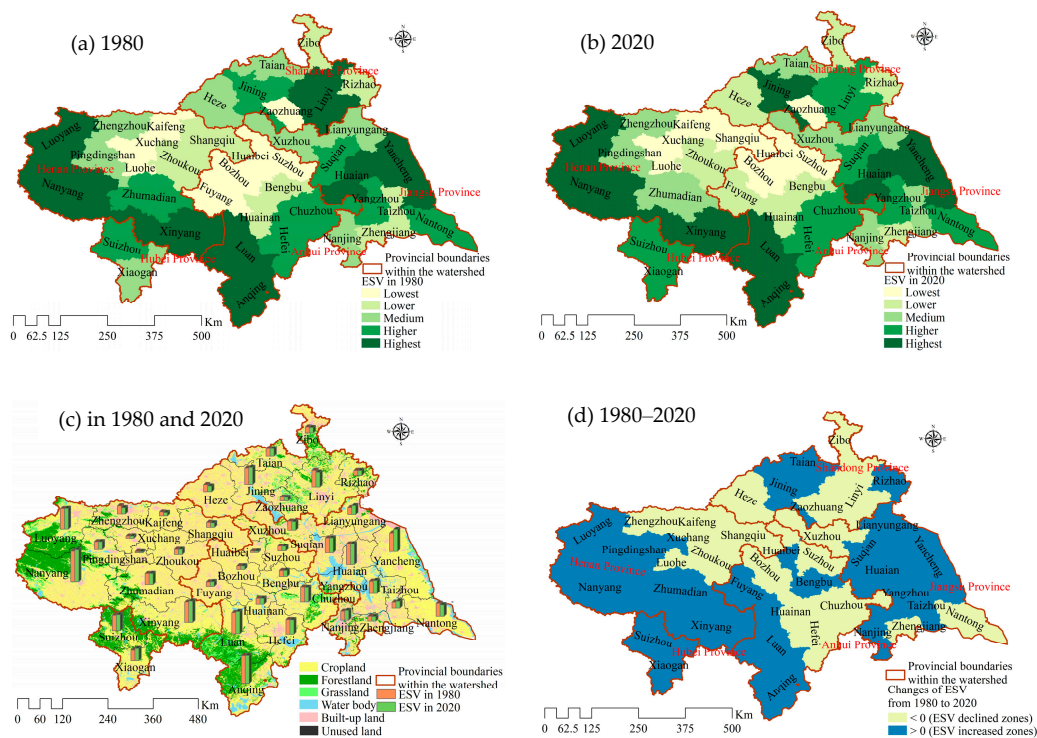
Figure 5. The spatial characteristics of ESV (**a**,**b**), ESV comparison (**c**), and ESV change (**d**) in the HRB from 1980 to 2020.

Analyses reveal that the change in ecosystem services was manifested as "continuous growth in the high-value areas and continuous decline in the low-value areas" from 1980 to 2020 in the HRB, which should attract the attention of the government; relevant measures should be implemented to curb the continuous decline in the value of ecological services in the central region and improve the overall ES value in the HRB.

3.1.2. Analysis of Changes in the New Urbanization

Over the past 40 years, the development of new urbanization in the HRB has increased steadily (Figure 6). A comprehensive urbanization index increased from 1.888 in 1980 to 11.524 in 2020, with an average annual growth rate of 12.76%, indicating a significant change. The comparison of urbanization development in different dimensions in the HRB shows that the level of population urbanization increased slowly, with an average annual growth rate of 5.47%, while the land urbanization level experienced the highest growth rate of 19.30%. The economic and social urbanization levels have also improved significantly, with annual growth rates of 14.10% and 17.85%, respectively. This indicates that the residents' medical and social security systems in the HRB have been further improved, the residents' well-being has improved, and the fruits of economic development in the basin have been shared.

There were distinct spatial differences in the new urbanization index (UI) of the HRB urban agglomerations. Among them, capital cities such as Zhengzhou, Hefei, and many cities of Jiangsu Province in the southeast show a notably high UI, while the urbanization index of cities in the central and western areas of the HRB remains low (Figure 7a,b), mainly because this region is an important base of agricultural production in China, with an overall low social and economic level and relatively weak impetus for infrastructure development. Figure 7c shows that the comprehensive index of urbanization of 40 cities in the HRB exhibited an upward trend, but the difference in growth rates remained significant. Figure 7d shows that from 1980 to 2020, the urbanization growth rate of 18 cities was lower than the overall average growth rate of urbanization in the HRB. Although the growth

rate of many cities with a low urbanization index in the central and western areas of the HRB was higher than the average growth rate, the overall distribution pattern of cities with low UI in the HRB remained unchanged. The analysis shows that the urbanization growth potential of cities in the middle and west parts of the basin is large, but the development momentum is insufficient, and the gap is still obvious compared with developed cities. The government must address this issue by enhancing the radiation driving effect of key cities on surrounding cities with a low urbanization level and promoting the development of high-quality urbanization in the HRB.
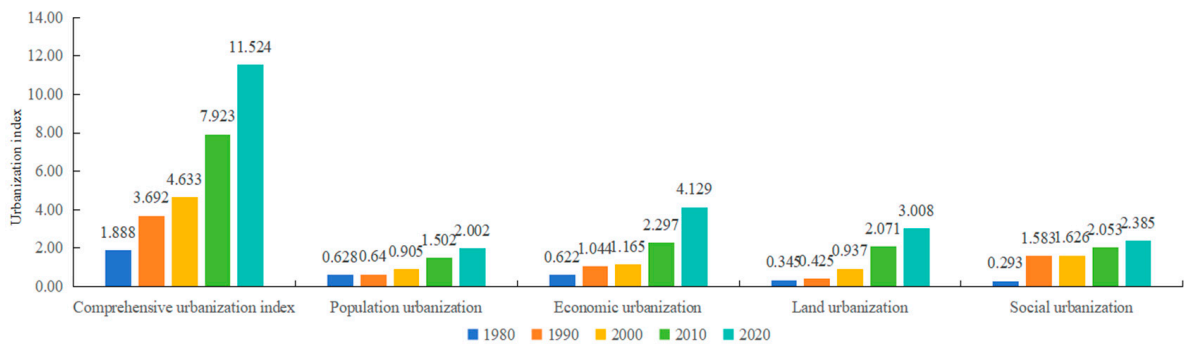
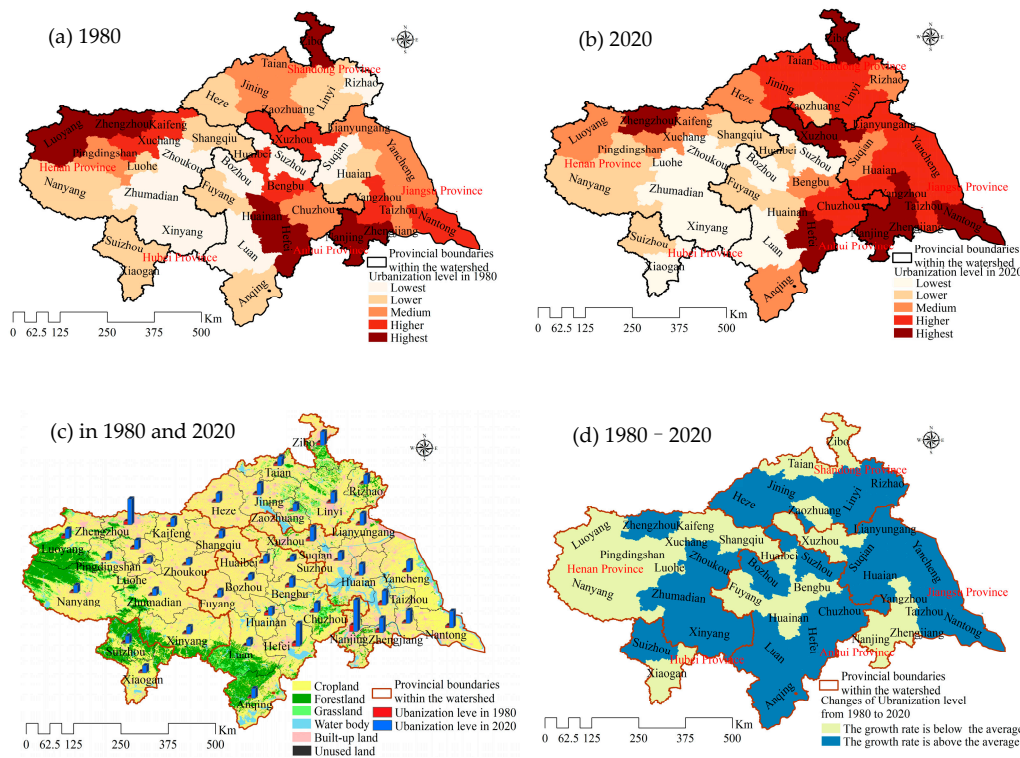**Figure 6.** The changing trend in urbanization development in the HRB from 1980 to 2020.

Figure 7. The spatial characteristic of the UI (**a**,**b**), UI comparsion (**c**), and UI change (**d**) in the HRB from 1980 to 2020.

3.2. Analysis of the Variation in CCD

3.2.1. The Trend and Characteristics of Spatio-Temporal Variation in CCD

From 1980 to 2020, the coupling relationship between the ES value and the urbanization index in the HRB showed an optimization trend year by year, and it went through four stages, namely moderate dysfunctionality, barely coordination, good coordination, and high-quality coordination, respectively (Table 6). During the study period, the CCD value increased from 0.260 in 1980 to 0.995 in 2020, an overall increase of 3.827 times, with an

average annual growth rate of 7.07%. The results show that the coupling degree (C) in 2000 reached 0.991, but the coordination index (T) was still only 0.254, and the final D value was 0.502, which was in the barely coordination stage. However, after 2000, all the indicators increased significantly (Table 6), indicating that the relationship between the ESs and urbanization in the HRB before 2000 was still in the low-level coupling stage. The analysis shows that the HRB gradually formed a development pattern of "developing in protection and upgrading in development" during the process of ecological protection and new urbanization over the past 40 years.

Table 6. Coupling characteristics of ESs and new urbanization in the HRB.

Years	Coupling Degree (C)	Coordination Index (T)	Coupling Coordinative Development Degree (D)	Coupling Coordination Level
1980	0.289	0.234	0.260	moderate dysfunctionality
1990	0.432	0.102	0.210	moderate dysfunctionality
2000	0.991	0.254	0.502	barely coordination
2010	0.994	0.698	0.833	good coordination
2020	1.000	0.990	0.995	high-quality coordination

On the whole, the coupling state of ESs and the level of new urbanization development in the HRB have shown good development trends, and detailed examination of the coupling state of the 40 cities in the basin can provide more specific guidance for urban development. Figure 8 shows the absolute amount of CCD (the calculated value) compared with the relative amount (the change, obtained by subtracting the 1980 CCD value from the 2020 CCD value) for the 40 cities in the basin. The absolute amounts of CCD in 1980 and 2020 show that most cities in Jiangsu Province and the capital cities of other provinces, such as Zhengzhou and Hefei, exhibited a high level of coupled development (Figure 8a).

Figure 8. Changes in the amount of the absolute (**a**) and the relative CCD (**b**) in 40 cities from 1980 to 2020.

The relative amount of CCD over the past 40 years indicates that 18 of the 40 cities in the basin showed a growing trend, accounting for 50% of the total number of growth cities, mainly located in Jiangsu Province. It is worth noting that Lu'an city in the Dabie Mountain area in Anhui Province led the increase in the CCD, reflecting that the ecological function of the Dabie Mountain area and the level of urbanization have a good coupling and collaborative development trend. There were 21 cities with a declining trend in CCD, mainly concentrated in Henan Province and Anhui Province, accounting for 52.38% and 28.57% of the total number of cities with a declining CCD, respectively, among which Huainan city in Anhui Province and Luoyang city in Henan Province showed the largest decline in CCD (Figure 8b).

3.2.2. Coupling Coordinated Development Degree Shifts and Spatial Heterogeneity

Upon calculating the CCD for the panel data from 40 prefecture-level cities in the HRB from 1980 to 2020, we used a chordal diagram to illustrate the shifts in the CCD for each city (Figure 9). Notably, the chordal diagram vividly shows a trend where more cities transitioned from a higher to a lower rank of coordinated development compared to those moving in the opposite direction. Although the CCD of the HRB cities mainly shifted from dysfunctionality to coordination types, most of them transitioned between lower-ranked coordination types, and there were fewer drastic shifts, such as from severe dysfunctionality to high-quality coordination, or from high-quality coordination to severe dysfunctionality, and most of the rank shifts were smoother. Therefore, although the entire HRB has shown excellent coupling coordination over the last 40 years, there is still a need to improve the quality and level of coupling in each prefecture-level city.
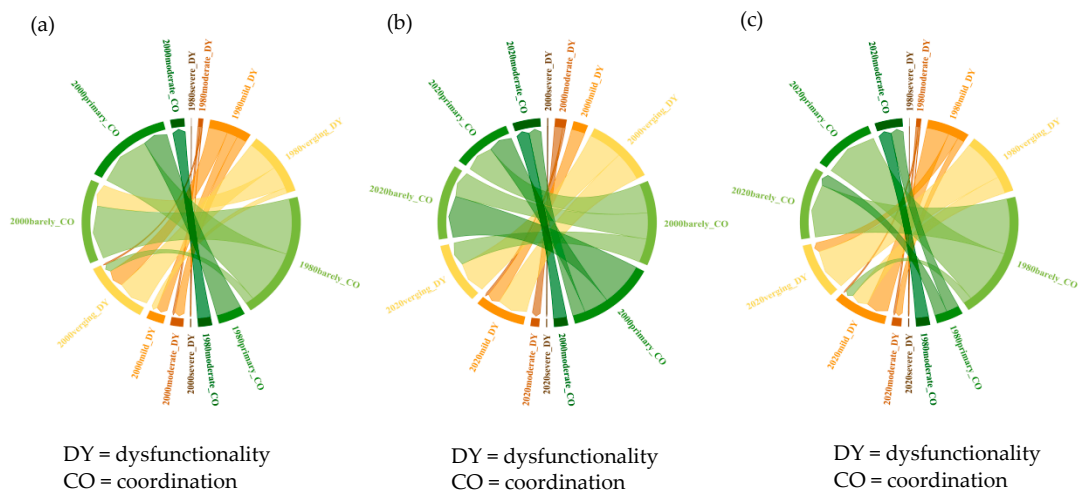

Figure 9. Chordal diagram of the CCD transition at 3 stages from 1980 to 2000 (**a**), from 2000 to 2020 (**b**), and from 1980 to 2020 (**c**) in the HRB.

In terms of spatial patterns (Figure 10), the low-value area of CCD was primarily located in the north-central region of the watershed, while the high-value area was dispersed across the capital cities, such as Nanjing, Hefei, and Zhengzhou, as well as in southeastern cities (Figure 10a,b).

According to the spatial distribution of CCD variation, 18 cities showed a CCD variation greater than 0, mainly located in the southeast part of the HRB, while there were 22 cities with a CCD variation less than 0, accounting for 55% of the total number of cities, mainly located in the middle and west parts of the HRB (Figure 10c). An exploratory spatial data analysis (ESDA) revealed significant spatial clustering characteristics of the value of ecosystem services, the comprehensive index of urbanization, and the degree of coupling coordinated development over the past 40 years. Comparing 1980 and 2020, Moran's I

for the ES value increased from 0.4529 to 0.4723, reflecting a centralized trend in spatial distribution. Moran's I of the urbanization comprehensive index decreased from 0.2194 to 0.2032, indicating a shift toward polycentric and more discrete spatial distribution. Moran's I of the CCD increased from 0.3967 to 0.5190 (Figure 10d), significantly enhancing the spatial agglomeration characteristic. Hotspot analysis revealed that the cold spot area of the CCD was in the central region of the basin and showed a clustered distribution, while the scope of the hot spot area included the southeastern regions with a tendency to expand (Figure 10e,f). The spatial analysis effectively demonstrated the distribution pattern and spatial evolution trend of the coupling relationship between ESs and urbanization in the study area. From 1980 to 2020, the overall coupling coordination was optimized year by year. These results provide decision-making support for exploring changes in ecosystem functions and the coordination mechanism of urbanization in the HRB in a precise manner.
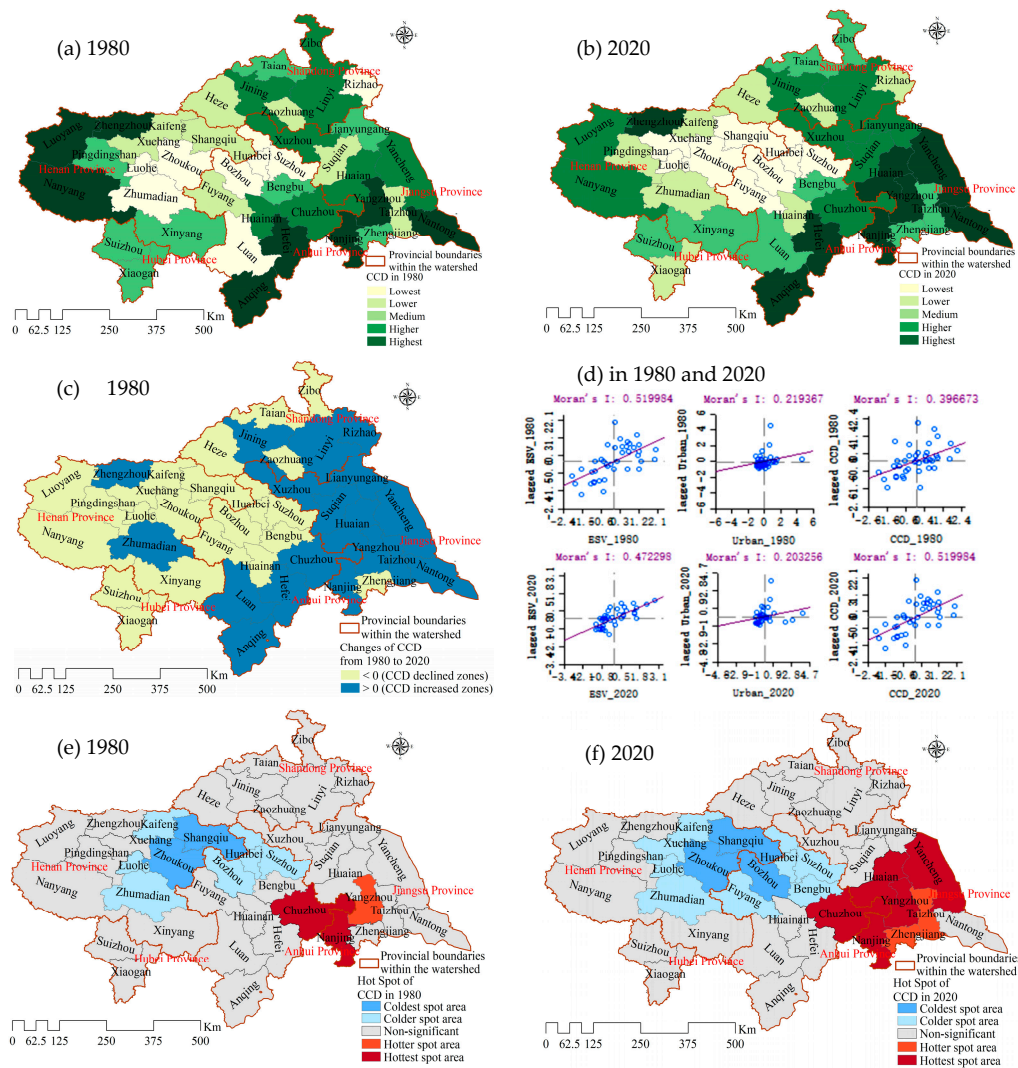

Figure 10. The spatial characteristic of the CCD (**a**,**b**). The change characteristics of CCD (**c**). Moran's *I* of ESV, UI and CCD in the HRB from 1980 to 2020 (**d**). The CCD Hot Spot analysis (**e**,**f**).

The analysis shows that the interaction between ESs and new urbanization in the HRB is complex and presents significant challenges, directly affecting the formulation and implementation of regional sustainable development strategies. First, there is an inconsistency between ecosystem services and urbanization. In some areas, urbanization leads to the degradation of ecosystem services, while in others, an excessive protection of ecosystems may restrict urban expansion. This results in imbalances in regional development, compli-

cating resource management and policy formulation. Second, the long-term persistence of low-level coupling between ecological protection and urbanization hinders their coordinated development, which ultimately affects the overall sustainability of the basin. Third, urban units in different provinces with a good coupling level exhibited varying trends in CCD changes throughout the study period. Some continued to improve, while others showed the opposite trend. Therefore, enhancing the coupling between ecological protection and urbanization is crucial for the successful implementation of regional sustainable development strategies. In this context, differentiated management strategies are essential.

Further analysis of the spatial statistical descriptors revealed that in 1980, the HRB had a minimum CCD value of 0.175 and a maximum value of 0.716, with a standard deviation (STDEV) of 0.129; in 2020, these values changed to 0.145, 0.726, and 0.146, respectively. The STDEV of the CCD increased from 0.129 to 0.146, indicating an expansion in the spatial disparities in the CCD among cities in the HRB (Table 7). According to the statistics of ESV and UI, the ESV showed relatively minor spatial disparity changes, with STDEV values of 0.343 and 0.360 in 1980 and 2020, respectively. However, the STDEV values for UI were 0.027 and 0.146 in 1980 and 2020, respectively (Table 7), which is the primary reason for the widening spatial disparities in the CCD. Against the backdrop of high-quality development in the HRB, it is necessary to further enhance the overall level of new urbanization in the central and western cities.

Table 7. Spatial statistical descriptors for ESV, UI, and CCD.

Year	Statistical Description of ESV at City Level				Statistical Description of UI at City Level				CCD Statistical Descriptors at City Level			
	Min	Max	Mean	STDEV	Min	Max	Mean	STDEV	Min	Max	Mean	STDEV
1980	0.059	1.440	0.504	0.343	0.019	0.157	0.047	0.027	0.175	0.716	0.440	0.129
2020	0.053	1.511	0.512	0.360	0.047	0.864	0.288	0.146	0.145	0.726	0.436	0.146

3.2.3. GeoDetection Analysis of the CCD

(1) Factor detection of spatial heterogeneity and its underlying mechanisms

Heterogeneity is a spatial feature in the interaction between natural factors and human activity factors, and human beings can understand and recognize natural phenomena through the analysis of spatial heterogeneity. GeoDetector-based methods can effectively reveal the driving mechanism of spatial heterogeneity in the CCD between the ES value and new urbanization. The contribution of driving factors to the spatial differentiation can reflect the interconnectivity between the factors and can also identify the importance of each factor to the spatial differentiation [41].

The calculation results indicate that among the 11 selected driving factors, 4 passed the significance test at the 1% level, 3 passed at the 5% level, and 4 passed at the 10% level (Figure 11a). As can be seen in Figure 11a, the spatial heterogeneity of the CCD between the ecosystem service value and urbanization in the HRB is affected by the combined effect of natural factors and socioeconomic factors, in which factors such as the average annual precipitation (AAP), distance from water body (Dwater), elevation, and GDP per area have a greater impact on the spatial heterogeneity of the CCD, while factors such as the distance from the railroad (Drailroad) and the annual average temperature (AAT) make relatively weak contributions to it. The factors in this study were sorted by the magnitude of *q*-statistics as follows: AAP > Dwater > DEM > GDP per area > aspect > slope > population density > total population > soil type > AAT > Drailroad (Figure 11a). Therefore, in terms of the influence of driving factors on the CCD, the explanatory abilities of AAP, Dwater, elevation, and GDP per area exceed 40%, making them the most significant, followed by aspect and slope, whose influences are around 30%, indicating that they are

important factors affecting the spatial variation in the CCD. The analysis suggests that AAP directly influences water availability, which is critical for ESs such as water conservation, agricultural production, and ecological restoration. In regions with abundant rainfall, water resources are sufficient, promoting ecosystem stability and enhancing ecosystem service functions, thereby facilitating the coordinated development of urbanization and ecological protection. Proximity to water bodies also plays a vital role, as areas near rivers, lakes, and other water bodies typically have higher environmental quality, better water quality, and are more suitable for eco-tourism and urban green spaces. In addition, population density, total population, and soil type all have an influence of more than 15%, signifying that they are more important factors that affect the spatial characteristic of the CCD. The explanatory abilities of AAT and Drailroad are below 10%, indicating their relatively minor influence on the spatial variation in the CCD.

(2) Interactive detection between driving factors

Using driving factor interaction detection, the spatial differences in the CCD within the HRB were revealed, showing that the interaction of any two factors is more significant than that of a single factor. The two-by-two interaction types mainly involve interaction-enhanced and nonlinear-enhanced interactions, indicating that the spatial differentiation of the CCD in the HRB is not solely attributed to a single influencing factor. Instead, it is the outcome of the combined action of various influencing factors. Among these interactions, the interaction between X_1 and X_{10} exerts the strongest effect on the spatial differentiation of the CCD, with the highest q-value of factor interaction detection reaching 0.980, providing a 98% explanatory power. The degree of interaction on the role of coupling coordinated spatial differentiation surpasses 90%. Other significant interactions include GDP per area ∩ Distance from water body (q-value 0.969), GDP per area ∩ Aspect (q-value 0.968), Soil type ∩ Distance from railroad (q-value 0.954), Total population ∩ Aspect (q-value 0.936), DEM ∩ Aspect (q-value 0.931), Population density ∩ GDP per area (q-value 0.928), GDP per area ∩ Aspect (q-value 0.925), GDP per area ∩ Average annual precipitation (q-value 0.912), GDP per area ∩ DEM (q-value 0.907), and DEM ∩ Distance from railroad (q-value 0.907) (Figure 11b).
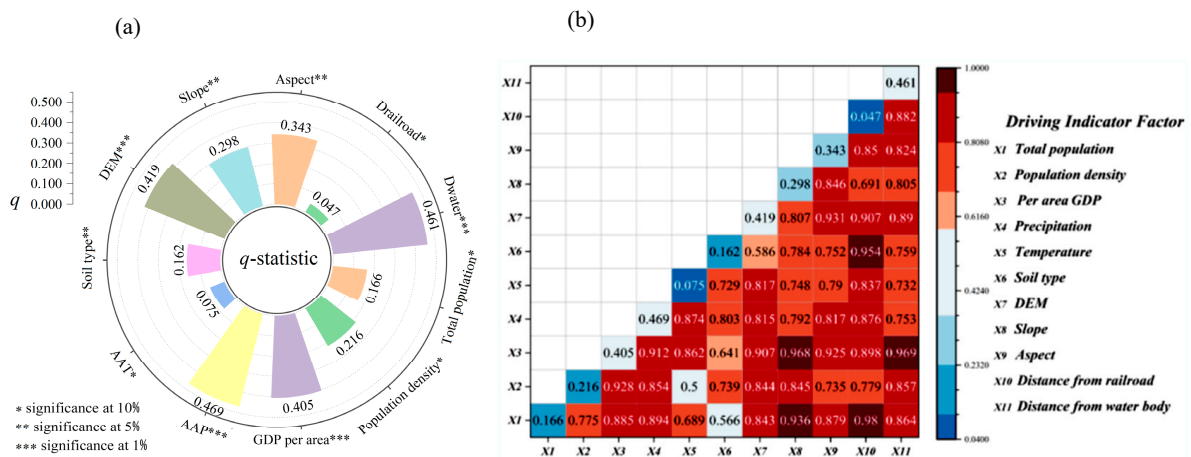

Figure 11. The results of factor detector (**a**) and interaction detector (**b**) for the CCD.

The q-values of the remaining factor interaction types are all below 50%, yet they still indicate the impact of the two-factor-higher degree of influence on the spatial differentiation of the CCD compared to the single factor (Figure 11b). The analysis reveals that all interactions between the driving factors of spatial divergence in the CCD in the HRB are more influential than the effect of a single factor.

3.3. Multi-Scenario Simulations of Land Use and ES Value

3.3.1. Analysis of Land Use Simulation

Using ArcGIS software, land use data from the initial and final years were reclassified, assigning values from 1 to 6 to six land classes. The simulation data of land use in 2020 obtained by using the PLUS model was compared with actual data, yielding a Kappa coefficient of 0.9211 and an overall accuracy of 92.11%. Although most studies on land use change simulation primarily use the Kappa coefficient to evaluate simulation accuracy, FoM indicators are increasingly used to assess the accuracy of land use simulations at the basin scale [39]. In this study, a FoM value of 0.052 was obtained using the FoM calculation tool in the PLUS model for land use simulation. The FoM coefficient theoretically ranges from 0.01 to 0.59, with higher values indicating greater simulation accuracy. Values below 0.30 are more commonly observed [42]. Therefore, based on both the Kappa and FoM coefficients, the land use simulation results in this study are considered to meet the necessary criteria. Next, we took 2010–2020 as the research base period and applied the PLUS model to simulate the land use data for 2050 according to the four scenarios (ND, CP, EP, and CD) designed in this paper (Table 8).

Table 8. Simulation results of land use data in 2050 under four scenarios.

	Cropland	Forestland	Grassland	Water Body	Built-Up Land	Unused Land
Area in 2020	249,910.88	46,369.39	14,778.18	22,885.91	58,187.63	356.28
ND 2050/km^2	230,350.34	45,310.19	15,162.83	24,227.58	77,135.40	301.93
CP 2050/km^2	258,477.03	45,707.23	12,859.19	21,124.81	54,020.45	299.56
EP 2050/km^2	241,999.47	48,724.68	14,299.84	23,773.53	63,382.33	308.42
CD 2050/km^2	236,261.83	45,392.29	14,330.44	24,558.84	71,648.08	296.79
ND 2050 (compared to 2020, %)	−7.83	−2.28	2.60	5.86	32.56	−15.25
CP 2050 (compared to 2020, %)	3.43	−1.43	−12.99	−7.70	−7.16	−15.92
EP 2050 (compared to 2020, %)	−3.17	5.08	−3.24	3.88	8.93	−13.43
CD 2050 (compared to 2020, %)	−5.46	−2.11	−3.03	7.31	23.13	−16.70

Note: ND = natural development; CP = cropland protection; EP = ecological protection; CD = comprehensive development.

Land use in 2050, compared to 2020, remains stable in cropland and forestland across all scenarios. Under ND, built-up land expands significantly, which emphasizes the need for policy intervention to prevent encroachment on ecological and agricultural land. CP reduces grassland and water body areas, affecting ecosystem services. EP protects ecological land, which aligns with regional policies, while CD increases built-up land and water body areas, emphasizing the need for careful consideration of cropland preservation.

3.3.2. Multi-Scenario Simulations of ES Value

Comparing land use changes across scenarios reveals significant differences (Figure 12), especially between cropland and built-up land in the scenario of CP and the scenario of ND. The expansion of patches in the HRB urban agglomeration decreases, and the mixing of cropland and forestland in the middle and lower plains decreases under CP, suggesting effective control over cropland shrinkage and the encroachment of forestland and built-up land. In the scenario of EP, the change rate of built-up land significantly decreases, and ecological land such as forestland and water body is effectively protected. This aligns positively with the policy of the Huaihe River Economic Zone, contributing to the ecological

security of the HRB. Under the scenario of CD, the water body area increased significantly, and the construction land area also increased, which enhanced the value of ecosystem services, safeguarding urban development. However, the decrease in cropland requires careful management to avoid compromising high-quality cropland. Strengthening land consolidation and reclamation is imperative to improve food productivity and ensure food security.

Changes in land use are a significant factor influencing the ES value in a region [43]. In comparison to the year 2020, by 2050, the total ES value under the CP scenario showed a notable decline, while values under the scenarios of ND, EP, and CD gradually increased. Research suggests that cropland primarily serves the purpose of food supply, yet its ecosystem service value is lower than that of grassland and water body. Furthermore, during the process of land use conversion, the increase in cropland area primarily comes at the expense of higher-value grassland and water body, causing a decline in the total ES value of the HRB. Therefore, while the CP scenario may promote an increase in cropland area, it negatively impacts the ecological protection of the HRB and poses significant risks to the region's water resource security. Against the backdrop of industrialization, urbanization, and climate change, this increases the level of land degradation and significantly impacts biodiversity loss, thus further threatening ecological security. The multi-scenario simulation illustrated the evolution of land use patterns and trends in ecosystem services under different policies. The results can provide scientific evidence for watershed management authorities to formulate strategies for ecological protection and urbanization development. Furthermore, the impact of land use changes on economic development under different scenarios can be analyzed, helping determine which land use practices are more conducive to economic growth.
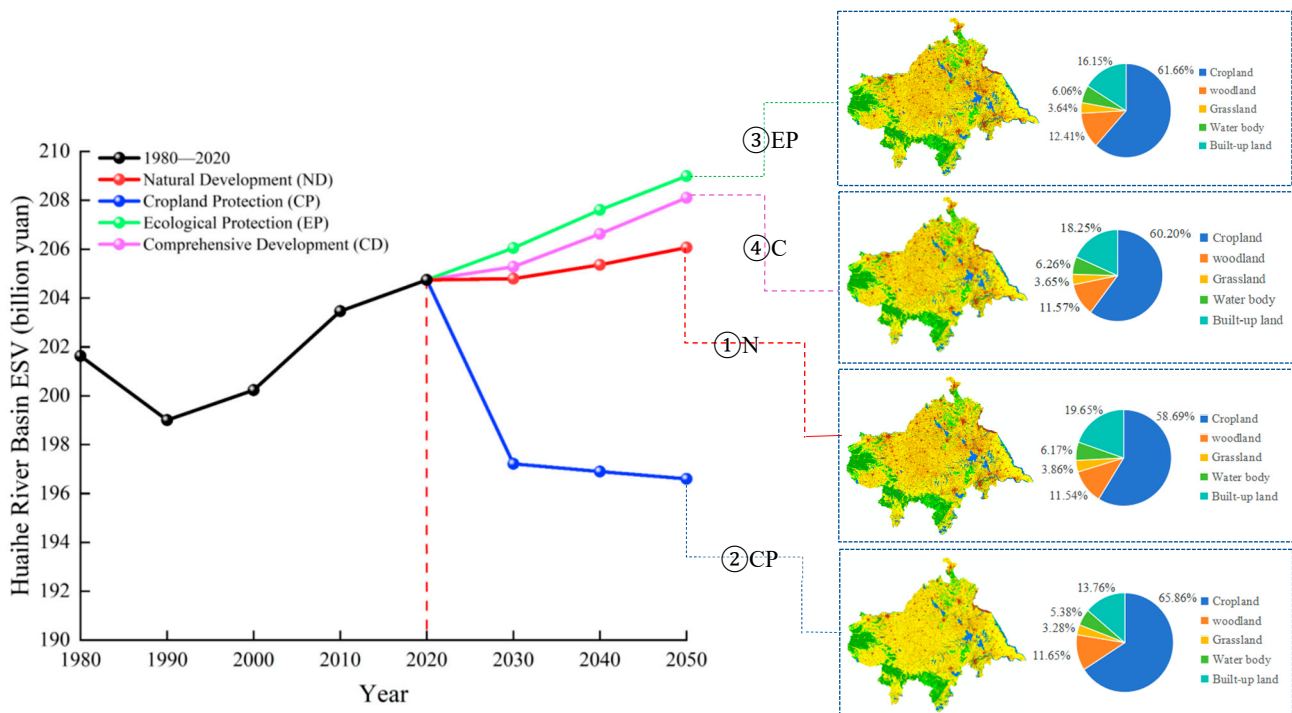

Figure 12. Trends in ecosystem service value under various scenarios from 1980 to 2050.

4. Discussion

4.1. Complex Interactions Between ESs, Urbanization, and Differentiated Regulation Strategies

ESs play a pivotal role in evaluating regional sustainable development, demanding a nuanced understanding of the mechanisms driving ecosystem functioning [44]. The

accelerated urbanization in China has led to evident environmental depletion, marked by the loss of cropland, declining biodiversity, and environmental pollution, particularly in urban agglomerations—regions now highly ecologically fragile and focal points for environmental treatment [45,46]. There is a complex coupling relationship between urbanization and the ecological environment [47], exhibiting both stage and spatial variability. Many researchers have quantified this coupling relationship, revealing patterns such as a double-exponential or inverted U-shaped curve [48]. However, the imbalance between urbanization and ecosystem services across different local areas in the watershed necessitates further exploration of the causes and driving mechanisms of this imbalance [49]. Differentiated and precise regulatory strategies are also required in the HRB.

The results show that CCD in the HRB has significant spatial differences, both in the scale of prefecture-level city units and provincial administrative units over the past 40 years. Therefore, the regulation and control of CCD in the HRB should adopt differentiated optimization measures. For example, in the eastern region, efforts should focus on further improving the quality of coupling state, while in the middle and western areas, the priority should be addressing shortcomings in the two coupling subsystems. Addressing the challenge of coordinated development between ecosystem services and urbanization requires comprehensive research into the value of ecosystem services and their strategic application in optimal land allocation. A differentiated regulatory strategy is crucial for promoting the coordinated development of ecosystem services and new urbanization in the HRB. This study introduces a strategy system based on "one framework, two methods, and three pathways" to address complex interactions and ensure the effective implementation and evaluation of these strategies.

The framework layer establishes a differentiated regulatory strategy tailored to the ecological characteristics, urbanization processes, and resource carrying capacities of various regions within the HRB. This framework aims to resolve conflicts between ecological protection and urbanization, promoting sustainable development across the basin. Two methods are employed to assess the effectiveness of the strategies: (1) qualitative methods, including expert evaluations, social surveys, and feedback from local governments and residents, to assess the acceptability and execution of the coordination between ecological protection and urbanization; (2) quantitative methods that use models such as the Synthetic Control Method (SCM) [50] to objectively assess the differentiated strategies across regions. Furthermore, the study proposes three implementation pathways: (1) the regional management pathway, which tailors goals based on local ecological and urbanization characteristics (e.g., water resource protection, wetland conservation), and establishes cross-regional collaboration mechanisms, ensuring coordinated governance across upstream and downstream areas; (2) the policy incentive pathway, which employs fiscal subsidies, tax incentives, and other policy measures to support green development, particularly in ecological restoration and green infrastructure projects; and (3) the technological innovation pathway, which promotes the application of green technologies, clean energy, and intelligent urban management systems to enhance ecological protection and improve the quality of urbanization.

4.2. Urbanization and Ecological Regulation Insights Based on Multi-Scenario Simulation

The HRB, positioned as the central link connecting the eastern and central parts of China, boasts good industrial infrastructure. However, the correlation among cities in the basin remains relatively loose. Over the nearly 40 years from 1980 to 2020, the cold spot area depicting the CCD remained largely unchanged, persisting in the central depression of the basin. Conversely, the coupling of urbanization and ecosytem services in southeastern cities has significantly improved. This indicates that major and core cities in the HRB have

limited influence on neighboring cities, resulting in insufficient coordination in resource use, environmental enhancement, industrial development, and socio-economic growth. Consequently, there is a lack of sufficient driving force in integrating urban and rural areas, improving urbanization quality, and addressing other related issues. This finding aligns with existing studies [51], suggesting that future research should leverage dynamic simulation technology to further explore the driving force and complexity of the coupling mechanism [52,53]. By simulating and predicting geographic processes historically, and with the support of algorithms such as long time series, multi-source big data fusion, and artificial intelligence, the complex evolutionary trends and dynamics between ecosystems and urbanization can be effectively revealed.

The simulation of ES value in 2050 was carried out by using the PLUS model. In comparison with 2020, the total ES value of the HRB in 2050 under the ND, EP, and CD scenarios increased gradually, while the total ES value under the CP scenario showed a decreasing trend. Under the EP scenario, the change rate of built-up land was significantly reduced, and ecological land such as forestland and water body could be effectively protected, contributing to the maintenance of ecological security in the HRB. Under the CD scenario, the area of water body with a high ES value and built-up land significantly increased, which enhanced the ES value and ensured the demand for urban construction land. However, there was a substantial reduction in cropland, highlighting the necessity to avoid destroying and occupying high-quality cropland. Strengthening land preparation and reclamation is crucial for improving food productivity and ensuring food security. These research findings offer valuable decision-making support for regulating ecosystem function and promoting high-quality development in the HRB.

4.3. Limitations of This Study and Potential Follow-Up Work

In this study, we comprehensively evaluated the ES value and the new urbanization index in the HRB from 1980 to 2020. Addressing the shortcomings of existing studies on the coupling of urbanization level and ecosystem services value, we detected the characteristics of the spatial heterogeneity of the coupling state and its driving force factors. Previous studies have also found that for watershed studies involving cross-administrative units, there is a need for in-depth exploration of how urbanization affects the ES value in different regions at multiple scales. Although our current study has obtained preliminary findings, in-depth and refined studies are still required. In addition, our study applies a multi-scenario simulation approach through the PLUS model and finally reveals the spatial characteristic of land use change in the HRB and predicted future trends for ecosystem service value in 2030, 2040, and 2050, respectively. These results provide insights into the dynamic evolution of land use and ES value in the HRB under different scenarios, which helps determine the future growth direction of urban boundaries for the regulation of ecosystem services [54]. The shortcomings of our study primarily include the lack of high data precision and a detailed analysis of the mechanisms influencing regional industrial layout development and ecosystem function. In future studies, we plan to strengthen the application of high-precision long-term data to obtain accurate and multi-scale data in the watershed. This will enable a more precise and diversified ecological management approach, providing decision-making support for the development of scientifically flexible spatial planning and industrial development layouts in the watershed.

5. Conclusions

Strengthening the exploration of the response and coupling mechanism of long-term ESs to urbanization development is of significant importance for ecological security and high-quality development in the HRB. This study introduces a new multidimensional

urbanization indicator system for the HRB, unveils the driving mechanisms behind the spatial heterogeneity of the CCD between new urbanization and ESs, and identifies the dominant factors. From 1980 and 2020, land use changes in the HRB followed a pattern of "four decreases and two increases." Over the 40-year period, the ES value in the HRB exhibited an initial decline followed by an upward trend, with 1990 marking a pivotal turning point. However, the growth rate of the ES value decelerated from 2010 to 2020. The comprehensive urbanization index exhibited consistent annual growth over the four decades, notably with a significant rise in the urbanization index of key cities such as Nanjing, Zhengzhou, and Hefei. The CCD between the ES value and new urbanization in the HRB progressed through varying stages of moderate dysfunction, barely coordinated, and high-quality coordinated, respectively. The CCD shows notable spatial clustering characteristics. These factors, such as precipitation, distance from water body, elevation, and per area GDP, emerge as the primary drivers of spatial disparities in the CCD. Simulation analysis forecasts a positive trajectory in the ES value from 2020 to 2050 under the scenarios of EP, CD, and NP. However, the scenario of CP indicates a certain degree of decline in the ES value. The results of the multi-scenario simulation analysis offer valuable insights into the formulation of a differentiated regulatory strategy in the HRB. The findings of this study are expected to assist watershed management authorities in better balancing ecological protection with urbanization.

Author Contributions: Conceptualization, M.H.; Methodology, M.H. and Q.G.; Formal analysis, Q.G. and G.Z.; investigation, Q.G., G.Z., Y.T. and X.W.; writing—original draft preparation, M.H. and Q.G.; writing—review and editing, M.H. and Q.G.; funding acquisition, M.H. All authors have read and agreed to the published version of the manuscript.

References

1. Qiao, X.; Zheng, J.; Yang, Y.; Liu, L.; Chen, Z. How does urbanization impact the supply–demand relationship of agroecosystem services? Insights from farmland loss in the Huaihe River Basin, China. *Ecol. Indic.* **2024**, *158*, 111406. [CrossRef]

2. Qian, X.; Wang, D.; Wang, J.; Chen, S. Resource curse, environmental regulation and transformation of coal-mining cities in China. *Resour. Policy* **2021**, *74*, 101447. [CrossRef]

3. Cheng, Z.; Li, L.; Liu, J. Natural resource abundance, resource industry dependence and economic green growth in China. *Resour. Policy* **2020**, *68*, 101734. [CrossRef]

4. Song, M.; Zhao, X.; Shang, Y.; Chen, B. Realization of green transition based on the anti-driving mechanism: An analysis of environmental regulation from the perspective of resource dependence in China, 2020. *Sci. Total Environ.* **2019**, *698*, 134317. [CrossRef]

5. You, M.; Zou, Z.; Zhao, W.; Zhang, W.; Fu, C. Study on land use and landscape pattern change in the Huaihe River Ecological and economic zone from 2000 to 2020. *Heliyon* **2023**, *9*, e13430. [CrossRef] [PubMed]

6. Jia, W.; Zhang, X.; Wang, Y. Assessing the pollutant evolution mechanisms of heavy pollution episodes in the Yangtze-Huaihe valley: A multiscale perspective. *Atmos. Environ.* **2021**, *244*, 117986. [CrossRef] [PubMed]

7. Costanza, R.; d'Arge, R.; de Groot, R.; Farber, S.; Grasso, M.; Hannon, B.; Limburg, K.; Naeem, S.; O'Neill, R.V.; Paruelo, J.; et al. The value of the world's ecosystem services and natural capital. *Ecol. Econ.* **1998**, *25*, 3–15. [CrossRef]

8. Alba-Patiño, D.; Carabassa, V.; Castro, H.; Gutiérrez-Briceño, I.; García-Llorente, M.; Giagnocavo, C.; Gómez-Tenorio, M.; Cabello, J.; Aznar-Sánchez, J.A.; Castro, A.J. Social indicators of ecosystem restoration for enhancing human wellbeing. *Resour. Conserv. Recycl.* **2021**, *174*, 105782. [CrossRef]

9. Hernández-Blanco, M.; Costanza, R.; Chen, H.; deGroot, D.; Jarvis, D.; Kubiszewski, I.; Montoya, J.; Sangha, K.; Stoeckl, N.; Turner, K.; et al. Ecosystem health, ecosystem services, and the well-being of humans and the rest of nature. *Glob. Change Biol.* **2022**, *28*, 5027–5040. [CrossRef]

10. Kibria, A.S.M.G.; Costanza, R.; Gasparatos, A.; Soto, J. A composite human wellbeing index for ecosystem-dependent communities: A case study in the Sundarbans, Bangladesh. *Ecosyst. Serv.* **2022**, *53*, 101389. [CrossRef]

11. Tapolczai, K.; Selmeczy, G.B.; Szabó, B.; B-Béres, V.; Keck, F.; Bouchez, A.; Rimet, F.; Padisák, J. The potential of exact sequence variants (ESVs) to interpret and assess the impact of agricultural pressure on stream diatom assemblages revealed by DNA metabarcoding. *Ecol. Indic.* **2021**, *122*, 107322. [CrossRef]

12. Zhang, S.; Sun, C.; Zhang, Y.; Hu, M.; Shen, X. Exploring the spatiotemporal changes and driving forces of ecosystem services of Zhejiang coasts, China, under sustainable development goals. *Chin. Geogr. Sci.* **2024**, *34*, 647–661. [CrossRef]

13. Li, J.; Zhang, Y. Coupling Coordination and Driving Factors of New-Type Urbanization and Ecological Efficiency in Yangtze River Delta Region. *Ecol. Econ.* **2022**, *38*, 109–114+141.

14. Zhai, Y.; Zhai, G.; Yu, Z.; Lu, Z.; Chen, Y.; Liu, J. Coupling coordination between urbanization and ecosystem services value in the Beijing-Tianjin-Hebei urban agglomeration. *Sustain. Cities Soc.* **2024**, *113*, 105715. [CrossRef]

15. Zhang, N.; Wang, Y. Study on the coupled coordination of new urbanization and water environment in the Yangtze River Economic Belt and its driving factors. *Resour. Environ. Yangtze Basin* **2024**, *33*, 572–583.

16. Zhang, S.; Huang, C.; Li, X.; Song, M. The spatial–temporal evolution and influencing factors of the coupling coordination of new-type urbanization and ecosystem services value in the Yellow River Basin. *Ecol. Indic.* **2024**, *166*, 112300. [CrossRef]

17. Pan, Z.; Gao, G.; Fu, B.; Liu, S.; Wang, J.; He, J.; Liu, D. Exploring the historical and future spatial interaction relationship between urbanization and ecosystem services in the Yangtze River Basin, China. *J. Clean. Prod.* **2023**, *428*, 139401. [CrossRef]

18. Tu, D.; Cai, Y.; Liu, M. Coupling coordination analysis and spatiotemporal heterogeneity between ecosystem services and new-type urbanization: A case study of the Yangtze River Economic Belt in China. *Ecol. Indic.* **2023**, *154*, 110535. [CrossRef]

19. Bi, Y.; Zheng, L.; Wang, Y.; Li, J.; Yang, H.; Zhang, B. Coupling relationship between urbanization and water-related ecosystem services in China's Yangtze River economic Belt and its socio-ecological driving forces: A county-level perspective. *Ecol. Indic.* **2023**, *146*, 109871. [CrossRef]

20. Wang, J.; Wang, Q.; Lu, D. Spatio-temporal coupling pattern and its influencing factors of digital economy, tourism economy and new urbanization: A case study of Yangtze River Delta region. *Geogr. Res.* **2024**, *43*, 3301–3326.

21. Li, Y.; Li, M. Coupling Coordination, Spatial–Temporal patterns and dynamic impact of the new urbanization and ecological resilience in the Yangtze River Economic Belt. *Resour. Environ. Yangtze Basin* **2024**, *33*, 2329–2341.

22. Chen, Y.; Cai, H.; Chen, Y. Spatial correlation and interaction effect intensity between territorial spatial ecological quality and new urbanization level in Nanchang metropolitan area, China. *Ecol. Indic.* **2023**, *156*, 111163. [CrossRef]

23. Yang, M.; Gao, X.; Siddique, K.H.; Wu, P.; Zhao, X. Spatiotemporal exploration of ecosystem service, urbanization, and their interactive coercing relationship in the Yellow River Basin over the past 40 years. *Sci. Total Environ.* **2023**, *858*, 159757. [CrossRef] [PubMed]

24. Xie, G.; Lu, C.; Leng, Y.; Zheng, D.; Li, S. Ecological assets valuation of the Tibetan Plateau. *J. Nat. Resour.* **2003**, *18*, 189–196.

25. Xie, G.; Zhen, L.; Lu, C.; Cao, S.; Xiao, Y. Supply, consumption and valuation of ecosystem services in China. *Resour. Sci.* **2008**, *30*, 93–99.

26. Huang, M.; Yue, W.; Fang, B.; Feng, S. Scale response characteristics and geographic exploration mechanism of spatial differentiation of ecosystem service values in Dabie Mountain area, central China from 1970 to 2015. *Acta Geogr. Sin.* **2019**, *74*, 1904–1920.

27. Pan, G.; Xu, Y.; Yu, Z.; Song, S.; Zhang, Y. Analysis of river health variation under the background of urbanization based on entropy weight and matter-element model: A case study in Huzhou City in the Yangtze River Delta, China. *Environ. Res.* **2015**, *139*, 31–35. [CrossRef]

28. Sun, X. Green city and regional environmental economic evaluation based on entropy method and GIS. *Environ. Technol. Innov.* **2021**, *23*, 101667. [CrossRef]

29. Li, J.; Qiu, J.; Amani-Beni, M.; Wang, Y.; Yang, M.; Chen, J. A modified equivalent factor method evaluation model based on land use changes in Tianfu New Area. *Land* **2023**, *12*, 1335. [CrossRef]

30. Cai, J.; Li, X.; Liu, L.; Chen, Y.; Wang, X.; Lu, S. Coupling and coordinated development of new urbanization and agro-ecological environment in China. *Sci. Total Environ.* **2021**, *776*, 145837. [CrossRef] [PubMed]

31. Sui, G.; Wang, H.; Cai, S.; Cui, W. Coupling coordination analysis of resources, economy, and ecology in the Yellow River Basin. *Ecol. Indic.* **2023**, *156*, 111133. [CrossRef]

32. Dong, G.; Ge, Y.; Liu, J.; Kong, X.; Zhai, R. Evaluation of coupling relationship between urbanization and air quality based on improved coupling coordination degree model in Shandong Province, China. *Ecol. Indic.* **2023**, *154*, 110578. [CrossRef]

33. Shi, S.; Wang, X.; Hu, Z.; Zhao, X.; Zhang, S.; Hou, M.; Zhang, N. Geographic detector-based quantitative assessment enhances attribution analysis of climate and topography factors to vegetation variation for spatial heterogeneity and coupling. *Glob. Ecol. Conserv.* **2023**, *42*, e02398. [CrossRef]

34. Wang, J.; Xu, C. Geodetector: Principle and prospective. *Acta Geogr. Sin.* **2017**, *72*, 116–134.

35. Liang, X.; Guan, Q.; Clarke, K.C.; Liu, S.; Wang, B.; Yao, Y. Understanding the drivers of sustainable land expansion using a patch-generating land use simulation (PLUS) model: A case study in Wuhan, China. *Comput. Environ. Urban Syst.* **2021**, *85*, 101569. [CrossRef]

36. Fu, F.; Jia, X.; Zhao, Q.; Tian, F.; Wei, D.; Zhao, Y.; Zhang, Y.; Zhang, J.; Hu, X.; Yang, L. Predicting land use change around railway stations: An enhanced CA-Markov model. *Sustain. Cities Soc.* **2024**, *101*, 105138. [CrossRef]

37. Niu, T.; Xiong, L.; Chen, J.; Zhou, Y.; Yin, J. Land Use Change Simulation and Multi-Scenario Prediction of the Yangtze River Basin based on the PLUS model. *J. Wuhan Univ. Technol.* **2024**, *57*, 129–141+151.

38. Li, H.; Fang, C.; Xia, Y.; Liu, Z.; Wang, W. Multi-scenario simulation of production-living-ecological space in the Poyang Lake area based on remote sensing and RF-markov-FLUS model. *Remote Sens.* **2022**, *14*, 2830. [CrossRef]

39. Lin, J.; Chen, Q. Analyzing and simulating the influence of a water conveyance project on land use conditions in the Tarim River region. *Land* **2023**, *12*, 2073. [CrossRef]

40. Pontius, R.; Boersma, W.; Castella, J. Comparing the input, output, and validation maps for several models of land change. *Ann. Reg. Sci.* **2008**, *42*, 11–37. [CrossRef]

41. Cui, F.; Wang, Y.; Liu, G. Exploring the spatial–temporal evolution and driving mechanisms for coupling coordination between green transformation of urban construction land and industrial transformation and upgrading: A case study of the urban agglomeration in the middle reaches of the Yangtze River. *Environ. Sci. Pollut. Res.* **2023**, *30*, 119385–119405.

42. Zhang, S.; Zhong, Q.; Cheng, D.; Xu, C.; Chang, Y.; Lin, Y.; Li, B. Landscape ecological risk projection based on the PLUS model under the localized shared socioeconomic pathways in the Fujian Delta region. *Ecol. Indic.* **2022**, *136*, 108642. [CrossRef]

43. Feng, Q.; Zhao, W.; Duan, B.; Hu, X.; Cherubini, F. Coupling trade-offs and supply-demand of ecosystem services (ES): A new opportunity for ES management. *Geogr. Sustain.* **2021**, *2*, 275–280. [CrossRef]

44. Qiao, X.; Gu, Y.; Zou, C.; Wang, L.; Luo, J.; Huang, X. Trade-offs and synergies of ecosystem services in the Taihu Lake Basin of China. *Chin. Geogr. Sci.* **2018**, *28*, 86–99. [CrossRef]

45. Ye, C.; Hu, M.; Lu, L.; Dong, Q.; Gu, M. Spatio-temporal evolution and factor explanatory power analysis of urban resilience in the Yangtze River Economic Belt. *Geogr. Sustain.* **2022**, *3*, 299–311. [CrossRef]

46. Zhang, G.; Wang, J.; Wu, K.; Xu, Z. Spatial-temporal characteristics and influencing factors of coordination between economic and environmental development of three major urban agglomerations in China. *Geogr. Res.* **2020**, *39*, 272–288.

47. Feng, Y.; He, S.; Li, G. Interaction between urbanization and the eco-environment in the Pan-Third Pole region. *Sci. Total Environ.* **2021**, *789*, 148011. [CrossRef] [PubMed]

48. Özokcu, S.; Özdemir, Ö. Economic growth, energy, and environmental Kuznets curve. *Renew. Sustain. Energy Rev.* **2017**, *72*, 639–647. [CrossRef]

49. Zhang, F.; Xu, N.; Wang, C.; Guo, M.; Pankaj, K. Multi-scale coupling analysis of urbanization and ecosystem services supply-demand budget in the Beijing-Tianjin-Hebei region, China. *J. Geogr. Sci.* **2023**, *33*, 340–356. [CrossRef]

50. Abadie, A.; Diamond, A.; Hainmueller, J. Synthetic control methods for comparative case studies: Estimating the effect of California's tobacco control program. *J. Am. Stat. Assoc.* **2010**, *105*, 493–505. [CrossRef]

51. Yao, X.; Chen, Y.; Sheng, Y.; Qi, H.; Zhang, Q.; Ou, C. Spatial and temporal evolution characteristics and influencing factors of coupling coordination degree of urbanization and eco-environment in the Huaihe Eco-economic Belt. *Res. Sq.* **2023**. [CrossRef]

52. Sui, Y.; Hu, J.; Zhang, N.; Ma, F. Exploring the dynamic equilibrium relationship between urbanization and ecological environment—A case study of Shandong Province, China. *Ecol. Indic.* **2024**, *158*, 111456. [CrossRef]

53. Tang, P.; Huang, J.; Zhou, H.; Fang, C.; Zhan, Y.; Huang, W. Local and telecoupling coordination degree model of urbanization and the eco-environment based on RS and GIS: A case study in the Wuhan urban agglomeration. *Sustain. Cities Soc.* **2021**, *75*, 103405. [CrossRef]

54. Liang, X.; Liu, X.; Li, X.; Chen, Y.; Tian, H.; Yao, Y. Delineating multi-scenario urban growth boundaries with a CA-based FLUS model and morphological method. *Landsc. Urban Plan.* **2018**, *177*, 47–63. [CrossRef]